JOURNAL OF SOLID STATE CHEMISTRY 88, 505–512 (1990)

High-Pressure Synthesis of $LiTiMF_6$ (M = Mn, Fe, Co, Ni) with Trirutile, Na_2SiF_6, and $PbSb_2O_6$ Structures

TOHRU SEKINO, TADASHI ENDO,[1] TSUGIO SATO, AND MASAHIKO SHIMADA

Department of Molecular Chemistry and Engineering, Faculty of Engineering, Tohoku University, Aoba-ku, Sendai, Miyagi 980, Japan

Received January 29, 1990

High- and low-pressure forms of $LiTiM^{2+}F_6$ (M^2 = Mn, Fe, Co, and Ni) were prepared by the reaction of LiF, TiF_3, and MF_2 under conditions of 1.5–7.0 GPa and 700–1200°C. All the low-pressure phases belonged to a trirutile structure. On the other hand, the high-pressure phases crystallized in a Na_2SiF_6-type structure for M^{2+} = Mn and a $PbSb_2O_6$-type structure for M^{2+} = Fe, Co, and Ni. According to the Rietveld analysis, it was observed that such structures were basically described as hexagonal close packing of F^- ions with cations placed in half of the octahedral sites, but involved a significant difference in cationic proportions at the z = 0 and 1/2 levels. Detailed structure data of high- and low-pressure phases are included in the present paper, and the structural stability of each phase is discussed relative to the synthetic P–T conditions.

Introduction

Pressure-induced transformation of MF_2 (M = divalent cation) with the rutile-type structure has been studied for many decades (*1*), because the high pressure form of SiO_2, stishovite, is an analog of rutile. Also, such transformation sequences were fairly useful to understand the internal structure of the earth. The unit cell of the rutile structure consists of two nonequivalent M^{2+} ions. Each of these M^{2+} ions is surrounded by an axially compressed F^- octahedron, so that the local symmetry of a M^{2+} site is only of orthorombic symmetry (*2*). Nevertheless, the structure corresponds to an overall tetragonal symmetry with space group $P4_2/mnm$. On the other hand, the trirutile structure is composed of more complicated surroundings of cations, because it involves a large number of cations with different charges. However, the space group is identical with that of the rutile structure. Also, only the c parameter of the unit cell is multiplied by 3 due to the additional ordering of some cations in every three layers.

Transition metal fluorides Li(Na) $M^{2+}M^{3+}F_6$ have various structural forms: trirutile, modified pyrochlore, tetragonal bronze, trigonal Na_2SiF_6, and so on. Recently, Gaile *et al.* (*3*) reported that Li $MnTiF_6$, $LiMnVF_6$, and $LiFeGaF_6$ changed structure from trirutile type to Na_2SiF_6 type at 595–650°C. Also, Courbion *et al.* (*4*) indicated that $LiMnFeF_6$ showed dimorphism at 560°C from α to β phases. The structural

[1] Present address: Department of Molecular Chemistry and Engineering, Faculty of Engineering, Tohoku University, Aoba-ku, Sendai, Miyagi 980, Japan.

0022-4596/90 $3.00

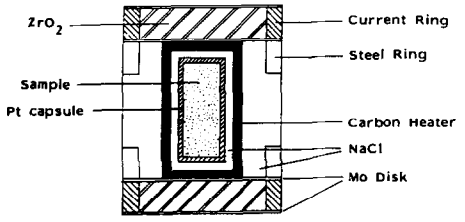

FIG. 1. Schematic drawing of the high-pressure cell assembly.

difference between the α and β phases was mainly due to an inversion between alkali and trivalent ions (Fe^{3+}) in the Na_2SiF_6 structure. However, pressure effects on the phase transformation of Li(Na)$M^{2+}M^{3+}F_6$ is still not well understood. Most of these structures consist of hexagonal close packing of F^- ions with octahedral sites for the cations. Accordingly, the cationic distribution and/or proportion in every layer is also responsible for the thermodynamic stability of the corresponding structure.

In this paper, the exact structure of Li TiMF_6 (M = Mn, Fe, Co, and Ni) is determined by using Rietveld X-ray refinements and the structural relationship with the synthetic P–T condition of each phase is discussed.

Experimental

Analytical grade LiF, TiF_3, and MF_2 (M = Mn, Fe, Co, and Ni) were purchased from Rare Metallic Co. Ltd (Tokyo, Japan) and Cerac/pure, Inc. (Wisconsin). These powders were weighed in stoichiometric proportions, intimately mixed under acetone, and dried at 100°C. In order to prevent the oxidation of the powder during the high-pressure experiment, the mixtures were uniaxially pressed under 200 MPa at room temperature and then sealed in a cylindrical gold capsule. The capsule was arranged in the high-pressure cell assembly as shown in Fig. 1, which consisted of a NaCl sleeve as the pressure medium and a carbon tube as the heater.

The reaction was carried out under the conditions of 1.5–7.0 GPa and 700–1200°C for 1–2 hr. Detailed information on the belt-type apparatus and its cell construction are described elsewhere (*5*). The sample was quenched within a few minutes to room temperature prior to the release of applied pressure. Temperatures were measured with a Pt/Pt–13% Rh thermocouple; the thermocouple emf was not corrected for pressure. The cell pressure was calibrated through monitoring the electrical changes due to the phase transformations of Bi(2.55 and 2.7 GPa) and Ba(5.5 GPa) at room temperature.

Powder X-ray diffraction data were obtained with a Shimazu XD-610 diffractometer system using Ni-filtered Cu$K\alpha$ or Fe-filtered Co$K\alpha$ radiation. Diffraction data were collected by step scan over an angular range of $10° < 2\theta < 100°$ in increments of 0.02° at room temperature. The $K\alpha_2$ component was stripped by the Rachinger method (*6*). A pseudo-Voigt profile function was used; the mixing parameter was included in the least-squares refinement. Peak positions were calibrated by using Si powder as an internal standard. Accurate unit cell parameters were calculated using a least-squares refinement method. Structure refinement of X-ray data was performed with the Rietveld analysis computer program RIETAN provided by Izumi (*7*).

The chemical compositions of the samples were determined by the Alfuson method described in the Ref. (*8*).

Results and Discussion

Dimorphism of LiTiMF$_6$

In the systems of LiF–TiF_3–MF_2 (M = Mn, Fe, Co, and Ni), two phases of LiTiMF_6 were observed depending on the reaction conditions; one was a phase with the tetragonal trirutile structure (referred to as trirutile type) and another was a phase indexed in hexagonal symmetry, which was derived from the trigonal Na_2SiF_6-related structures

TABLE I

CRYSTAL STRUCTURE AND LATTICE CONSTANTS OF LiTiMF$_6$ (M^{2+} = Mn, Fe, Co, AND Ni)

Composition	Lattice constants			
	a (nm)	c (nm)	$c/3a$[a]	V (nm^3)[b]
Trirutile	$\pm_{0.00007}$	$\pm_{0.0001}$		
LiTiMnF$_6$	0.4749	0.9536	0.6693	0.1076
LiTiFeF$_6$	0.4705	0.9481	0.6717	0.1049
LiTiCoF$_6$[c]	0.4682	0.9351	0.6657	0.1025
LiTiNiF$_6$[c]	0.4668	0.9216	0.6581	0.1004
Hexagonal	$\pm_{0.0001}$	$\pm_{0.00006}$		
LiTiMnF$_6$[c]	0.8799	0.4705	0.5347	0.1052
LiTiFeF$_6$	0.8707	0.4619	0.5347	0.1011
LiTiCoF$_6$[c]	0.8638	0.4589	0.5313	0.0988
LiTiNiF$_6$	0.8609	0.4548	0.5283	0.0973

[a] c/a value for Na_2SiF_6 type.
[b] Unit cell volume with one chemical formula per cell.
[c] Only a single phase is observed.

by the substitution $Na^+ + Si^{4+} \rightarrow M^2 + M^{3+}$ (referred to as hexagonal type). The X-ray diffraction data are summerized in Table I. The unit cell volume of hexagonal-type phase was 2.2–3.6% smaller than that of the trirutile-type phase. This implied that the hexagonal type phase was structurally stabilized under the high-pressure conditions. Figure 2 shows the yield of the resulting phases as a function of the synthetic pressure and the ionic radius ratio $r_{M^{2+}}/r_{Ti^{3+}}$ at 800°C. In the system of LiF–TiF_3–MnF_2, a single phase of trirutile type was not obtained, and a small amount of hexagonal type phase was formed at a pressure of 1.5 GPa. Both types of LiTiFeF$_6$ were also synthesized under 800°C and 3–6.5 GPa. However, it was difficult to crystallize both types in single phase LiTiFeF$_6$ at a temperature of up to 1200°C using the present mixture of starting materials. On the other hand, both types of the LiTiCoF$_6$ phases were prepared as single phases. In the LiF–TiF_3–NiF_2, the trirutile-type LiTiNiF$_6$ was synthesized at 3.0 GPa and 800°C as a single phase. The high pressure products synthesized at 7.0 GPa and 800°C consisted of the hexagonal-type phase as the main phase, but a small amount of tritutile-type phase was also present as second phase. Figure 2 suggested that the stable P–T regions of two type phases were closely governed by the size of M^{2+} ion for that of Ti^{3+} ion. However, the difficulties in obtaining single phase materials seemed to be mainly due to the small differences of the unit cell volume and a small deviation of composition between the two phases.

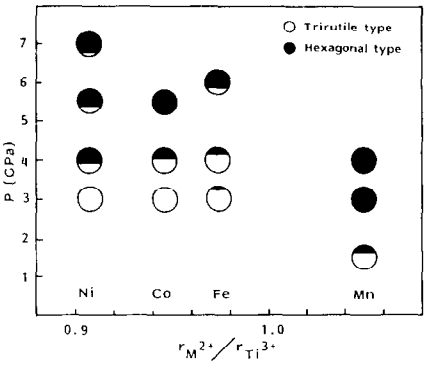

FIG. 2. Pressure-induced polymorphism of LiTiMF$_6$ as a function of the ionic radius ratio $r_{M^{2+}}/r_{Ti^{3+}}$ at 800°C.

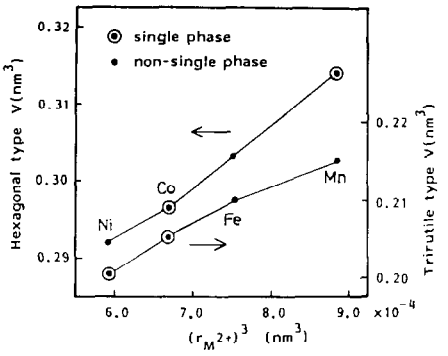

FIG. 3. Relationship between the cube of M^{2+} ionic radius and unit cell volume of $LiTiMF_6$. The radii are Ahrens ionic radii.

The relationship between the unit cell volume and the cube of M^{2+} ionic radii is shown in Fig. 3. Generally, the cell volume increased linearly with the ionic radius of the cation in the rutile structure. However, such a linear relationship was not observed in the present trirutile-type phases. This was mostly due to the site preference of Li^+, Ti^{3+}, or M^{2+} as will be described later.

In the system $LiF–TiF_3–CoF_2$, for which we obtained both types of $LiTiCoF_6$ as a single phase, the preparation of $(Li,Ti)_{1-x}Co_{1+2x}F_6$ was carried out by using a mixture of $(1 - x)LiF$, $(1 - x)TiF_3$, and $(1 + 2x)CoF_2$ as starting materials. Consequently, a trirutile-type phase, a rutile-type phase, and a hexagonal-type phase are systematically obtained as the function of x and pressure as shown in Fig. 4. When the chemical composition of the product deviated from stoichiometric $LiTiCoF_6$ ($x = 0$) toward $x < 0$, a hexagonal phase tended to be formed at lower pressure conditions. Whereas no trirutile-type and hexagonal-type phases were observed above $x = 0.2$, only a rutile-type phase was observed, whose lattice parameters were somewhat different from that of CoF_2. The existence of the rutile-type phase in the present solid–solution system was eventually achieved with excess of Co^{2+} ion, which occupied the Li or/and Ti ion sites at random. Also, the statistical ordering of cations rapidly decreased and the partial distortion of the CoF_6 octahedron simultaneously enhanced in both phases. Table II shows the crystal data of $(Li,Ti)_{1-x}Co_{1+2x}F_6$. This implied that the change of compositions resulted in changes of the lattice constants in the tritutile-type phase, but in the hexagonal-type phase. A similar structural change was observed in the system $(1 + x)(LiF–TiF_3–NiF_2$. Increasing the Li^+ content, the (002) and (101) peaks of X-ray diffraction, which was evidence for the trirutile-type phase, decreased in intensity. Above $x = 1$, the formation of a rutile-type phase was mostly due to the random distribution of the Li^+ ion.

The Crystal Structure of $LiTiMF_6$

Structure data on the trirutile type of $(Li,Ti)_{0.9}Ni_{1.2}F_6$. The expected trirutile structure was verified by the use of the Rietveld profile refinement method. Figure 5 shows the observed, calculated, and difference powder profile for $(Li,Ti)_{0.9}Ni_{1.2}F_6$. Also, Table III shows the atomic parameters and the isotropic temperature factors refined at 5.11% of the disagreement index, R_F. This data showed that Ni^{2+} was occupied on the 2*a* site and Li^+, Ti^{3+}, or excess of Ni^{2+} was distributed on the 4*e* site. The average ionic radius of $(Li^+ + Ti^{3+})/2$ was

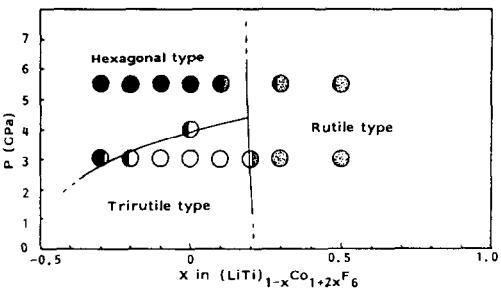

FIG. 4. Pressure-induced polymorphism at 750°C as a function of x in $(Li,Ti)_{1-x}Co_{1+2x}F_6$.

TABLE II

CRYSTAL STRUCTURE AND LATTICE CONSTANTS OF $(Li,Ti)_{1-x}Co_{1+2x}F_6$

Composition	Lattice constants			
	a (nm)	c (nm)	c/a	V (nm^3)
Trirutile	$\pm_{0.00006}$	$\pm_{0.0001}$		
$(Li,Ti)_{1-x}Co_{1+2x}F_6$				
$x = 0.01$	0.4686	0.9360	0.6658[a]	0.2055
$x = 0.0$	0.4682	0.9351	0.6657[a]	0.2050
$x = -0.1$	0.4681	0.9325	0.6640[a]	0.2043
$x = -0.2$	0.4674	0.9290	0.6625[a]	0.2030
Rutile	$\pm_{0.0001}$	$\pm_{0.0001}$		
CoF_2	0.4702	0.3176	0.6755	0.2107[c]
Hexagonal	$\pm_{0.00008}$	$\pm_{0.00007}$		
$(Li,Ti)_{1-x}Co_{1+2x}F_6$				
$x = 0.1$[b]	0.8636	0.4588	0.5313	0.2963
$x = 0.0$	0.8638	0.4589	0.5313	0.2965
$x = -0.1$	0.8635	0.4591	0.5317	0.2965
$x = -0.2$	0.8627	0.4589	0.5319	0.2958

[a] $c/3a$ value.
[b] No single phase is formed.
[c] $3V$ value.

calculated to be 0.0845 nm, which was almost the same as the ionic radius of Ni^{2+} (=0.084 nm) (*9*). Therefore, the regular distribution of such cations seemed to contribute to the stability of the structure. The nearest-neighbor bond distances of Ni(at 2*a* site)–F and *M*(at 4*e* site)–F were calculated to be 0.198 and 0.203 nm, respectively. The bond distance of Ni–F was relatively smaller than that of NiF_2 (0.201 nm) with rutile structure.

Structure data on the hexagonal-type $LiTiMnF_6$. According to the powder X-ray diffraction pattern, this phase was readily

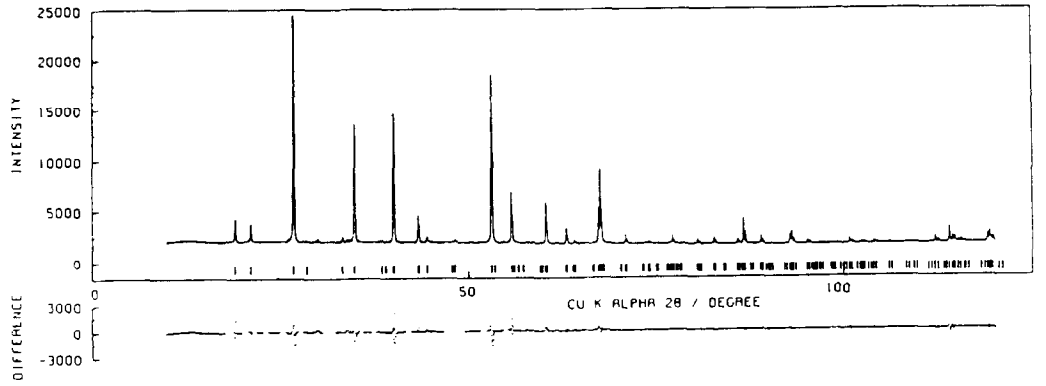

FIG. 5. Comparison between observed and calculated intensities of the powder X-ray diffraction peaks, and the difference pattern for $(Li,Ti)_{0.9}Ni_{1.2}F_6$.

TABLE III

REFINED CELL PARAMETERS AND ATOMIC COORDINATES OF $(Li,Ti)_{0.9}Ni_{1.2}F_6$

Space group: $P4_2/mnm$ (No. 136) $3a$ = 0.4664 (nm)
Z = 2 c = 0.9210 (nm)
$c/3a$ = 0.6582 v = 0.2006 (nm^3)

Atom	Site	x	y	z	B (Å^2)
2 Ni	2*a*	0	0	0	0.585
4 $Li_9Ti_9Ni_2$	4*e*	0	0	0.3316	0.730
4 F(1)	4*f*	0.2990	0.2990	0	0.945
8 F(2)	8*j*	0.3005	0.3005	0.3393	0.458

Note. R_I = 4.92%; R_F = 5.11%; R_{wp} = 5.65%; R_p, 3.70%.

identified as the Na_2SiF_6 structure in the $P321$ (No. 150) space group. Table IV shows the refined cell parameters and atomic coordinates of $LiTiMnF_6$. The (001) projection of $LiTiMnF_6$ configuration is illustrated in Fig. 6a. It could be seen that the cationic distribution was almost the same as that of α – LiF_6 reported by Courbion *et al.* (*4*). As shown in Fig. 6b, the structure consists of distorted hexagonal close packing of F^- ions with octahedral holes half occupied. In the level z = 0, 4/9 of the octahedral holes are filled; 1/9 by Li^+ ions and 1/3 by Mn^{2+} ions. The level z = 1/2 is occupied by Li^+ ions in 2/9 of the octahedral sites and Ti^{3+} ions in 3/9 of the octahedral sites. In addition, the present lattice parameters listed in Table IV were slightly smaller than those of $LiTiMnF_6$, a = 0.875_3 nm and c = 0.471_5 nm, prepared under the ambient pressure (*3*). In this context, the structure seemed to be readily quenched on keeping the pressure-induced distortions of the MF_6 octahedron. The average bond distances M–F for the MF_6 octahedron were calculated to be 0.246 nm for Li(1*a*), 0.233 nm for Li(2*d*), 0.225 nm for Mn^{2+}, and 0.192 nm for Ti^{3+}.

Structure data on the hexagonal type $(Li,Ti)_{1.2}Co_{0.6}F_6$. The X-ray diffraction patterns of $(Li,Ti)_{1.2}Co_{0.6}F_6$ was somewhat sim-

TABLE IV

REFINED CELL PARAMETERS AND ATOMIC COORDINATES OF $LiTiMnF_6$

Space group: $P321$ (No. 150) a = 0.8741 (nm)
Z = 3 c = 0.4700 (nm)
c/a = 0.5377 v = 0.3110 (nm^3)

Atom	Site	x	y	z	B (Å^2)
1 Li	1*a*	0	0	0	3.87
2 Li	2*d*	1/3	2/3	0.4114	1.63
3 Mn	3*e*	0.6464	0	0	1.54
3 Ti	3*f*	0.3111	0	1/2	0.644
6 F(1)	6*g*	0.8912	0.7526	0.3387	0.339
6 F(2)	6*g*	0.4672	0.5825	0.6873	4.44
6 F(3)	6*g*	0.2298	0.7566	0.2827	5.61

Note. R_I = 7.40%; R_F = 8.11%; R_{wp} = 3.58%; R_p = 2.58%.

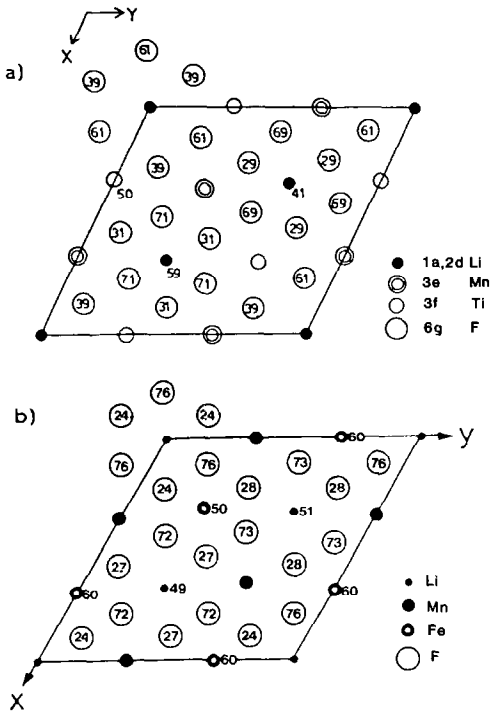

FIG. 6. (001) projection of (a) $LiTiMnF_6$ (this work) and (b) α-$LiFeMnF_6$ (*4*) absolute configuration.

TABLE V

POLYHEDRAL EDGE LENGTHS, BOND LENGTHS, AND MAIN DIFFERENT BOND ANGLES IN $(Li,Ti)_{1.2}Co_{0.6}F_6$

Octahedron of $Li_{0.83}Ti_{0.04}Co_{0.13}$ (1*a*): Symmetry 32	
6 × M1–F = 0.2082 nm	
F1–F2 = F2–F3 = F1–F3 = 0.2976 nm	F1–M1–F2 = 91.24°
F4–F5 = F5–F6 = F4–F6 = 0.2976	F4–M1–F5 = 91.24
F1–F2 = F2–F5 = F3–F6 = 0.2974	F1–M1–F4 = 91.16
F1–F5 = F2–F6 = F3–F4 = 0.2851	F1–M1–F5 = 86.44
Average distances: F–F = 0.2944 nm	
Octahedron of $Li_{0.37}Ti_{0.16}Co_{0.47}$ (1*e*): Symmetry 32	
6 × M2–F = 0.1970 nm	
F1–F2 = F2–F3 = F1–F3 = 0.2739 nm	F1–M2–F2 = 88.06°
F4–F5 = F5–F6 = F4–F6 = 0.2379	F4–M2–F5 = 88.06
F1–F5 = F2–F6 = F3–F4 = 0.2851	F1–M2–F5 = 92.69
F1–F6 = F2–F4 = F3–F5 = 0.2815	F1–M2–F6 = 86.44
Average distances: F–F = 0.2786 nm	
Octahedron of Ti (1*d*): Symmetry 32	
6 × Ti–F = 0.2024 nm	
F1–F2 = F2–F3 = F1–F3 = 0.2922 nm	F1–Ti–F2 = 92.40°
F4–F5 = F5–F6 = F4–F6 = 0.2922	F4–Ti–F5 = 92.40
F1–F4 = F2–F5 = F3–F6 = 0.2884	F1–Ti–F4 = 90.89
F1–F6 = F2–F4 = F3–F5 = 0.2721	F1–Ti–F6 = 84.48
Average distances: F–F = 0.2862 nm	
Superexchange distances and angles	
M1–M2 = 0.2877 nm	M1–F1–M2 = 90.43°
M1–Ti = 0.3680	M1–F2–Ti = 127.3
M2–Ti = 0.3680	M2–F5–Ti = 134.2

Note. Fluorine ions are noted by the number, F*i*. *i* refers to the coordinates of an equivalent positions as given in the order of International Tables.

pler than that of $LiTiMnF_6$ in space group *P*321. High pressure (hexagonal type) phases of stoichiometric $LiTiCoF_6$ and $LiTiNiF_6$ also gave the same profiles as described above. Accordingly, the refinements of the structure were carried out by using the space group *P*321 (No. 149), where the lattice parameters of *a* are 1/3 that of *a* in the Na_2SiF_6 structure. Figure 7 shows the observed and calculated intensities of powder X-ray diffraction peaks and the difference pattern for $(Li,Ti)_{1.2}Co_{0.6}F_6$ refined at 4.84% of R_F. The refined cell parameters and the atomic coordinates of

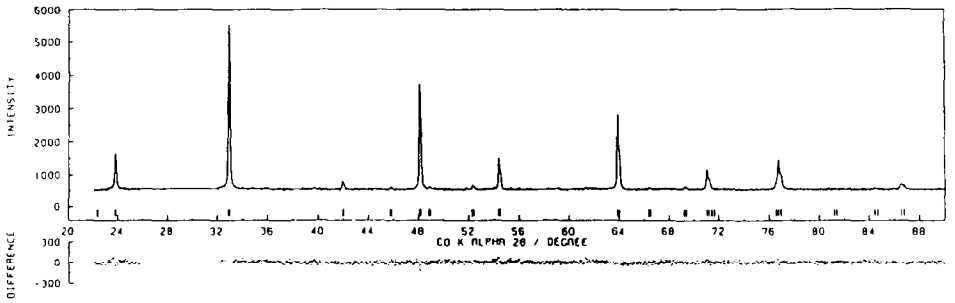

FIG. 7. Comparison between observed and calculated intensities of powder X-ray diffraction peaks, and the difference pattern for $(Li,Ti)_{1.2}Co_{0.6}F_6$ (R_F = 4.84%, R_{wp} = 4.56%).

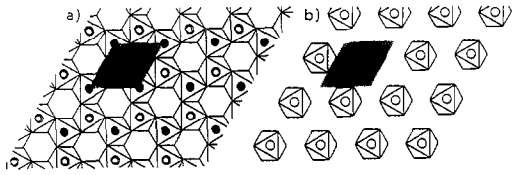

FIG. 8. Schematic representation of the edge-shared MF_6 octahedral network for $(Li,Ti)_{1.2}Co_{0.6}F_6$: (a) the layer $z = 0$ and (b) the layer $z = 1/2$. The unit cell is highlighted.

$(Li,Ti)_{1.2}Co_{0.6}F_6$ are listed in Table V. Also, the more significant M–F distances and bond angles of MF_6 octahedron are listed in Table V. Figure 8 represents the schematic illustration of an edge-shared MF_6 octahedral network on the $z = 0$ level and isolated MF_6 clusters on the $z = 1/2$ level. The present structure was basically derived from $PbSb_2O_6$ (space group $P312$) (*10*) or Li_2NbF_6 (space group $P31m$) (*11*), which consisted of a hexagonal close-packed anion array with the ordered cations occupying the octahedral sites. Figure 8 shows that 2/3 of Li^+, Ti^{3+}, and Co^{2+} ions are statistically located in the 1*a* and 1*e* sites at the level $z = 0$, and 1/3 of Ti^{3+} is only located in 1*d* sites at $z = 1/2$ level of $(Li,Ti)_{1.2}Co_{0.6}F_6$. The structure was different from the Na_2SiF_6 structure. The only major difference between the two types is due to the proportion of cations at each layer of $z = 0$ and $z = 1/2$; in other words, M^{2+} and Li^+ predominantly occupy similar positions.

Conclusions

Two kinds of structures are proposed as high pressure forms of $LiTiMF_6$ with trirutile structure. One is derived from the trigonal Na_2SiF_6 structure, which resulted in the different cationic distribution. Another is related to the $PbSb_2O_6$ structure with hexagonal symmetry, which was considerably different from the Na_2SiF_6 structure in the proportion of cations on every layer. It was seen that the ionic radius ratio $r_{M^{2+}}/r_{Ti^{3+}}$ is preferable to estimate the transformation sequences between the phases.

Acknowledgments

The present authors are indebted to the management of Showa Denko Co., Ltd. (Soga, Shiojiri, Nagano 399-64, Japan) for supporting several parts used for high-pressure experiments.

References

1. L. C. MING AND M. H. MANGHNAMI, *Geophys. Res. Lett.* **5,** 491 (1979); *Geophys. Res. Lett.* **6,** 13 (1979).
2. F. A. GRANT, *Rev. Mod. Phys.* **31,** 646 (1959).
3. VON J. GAILE, W. RUDORFF, AND W. VIEBAHN, *Z. Anorg. Allg. Chem.* **430,** 161 (1977).
4. G. COURBION, C. JACOBONI, AND R. DE PAPE, *J. Solid State Chem.* **45,** 127 (1982).
5. O. FUKUNAGA, S. YAMAOKA, T. ENDOH, M. AKAISHI, AND H. KANDA, "High Pressure Science and Technology" (K. D. Timmerhaus and M. S. Barber, Eds.), Vol. 1, p. 846, Plenum, New York (1979).
6. W. A. RACHINGER, *J. Sci. Instrum.* **25,** 254 (1948).
7. F. IZUMI, *J. Mineral. Soc. Japan* **17,** 37 (1985).
8. H. HASHITANI, H. YOSHIDA, AND H. MUTO, Japan Anal. **16,** 44 (1967).
9. L. H. AHRENS, *Geochim. Cosmochim. Acta.* **2,** 155 (1952).
10. H. VINCENT, X. TURRILLAS, AND I. RASINES, *Mater. Res. Bull.* **22,** 1369 (1987).
11. M. B. BOURNONVILLE, D. BIZOT, J. CHASSAING, AND M. QUARTON, *J. Solid State Chem.* **62,** 212 (1986).